NJC

ROYAL SOCIETY OF CHEMISTRY

PAPER

View Article Online
View Journal | View Issue

Check for updates

Cite this: *New J. Chem.*, 2022, **46**, 14826

Syntheses of novel fluorinated dibenzo[*a*,*c*]phenazine comprising polymers for electrochromic device applications

Serife O. Hacioglu, *[ab] Ece Aktas,[c] Gonul Hizalan,[d] Naime Akbasoglu,[b] Ali Cirpan [bde] and Levent Toppare [bef]

Received 6th June 2022,
Accepted 4th July 2022

DOI: 10.1039/d2nj02775e

rsc.li/njc

In this study, two novel fluorinated dibenzo[*a*,*c*]phenazine derivatives, 2,7-bis(5-bromo-4-hexylthiophen-2-yl)-11-fluorodibenzo[*a*,*c*]phenazine (TFBPz) and 2,7-bis(2,3-dihydrothieno[3,4-*b*][1,4]dioxin-5-yl)-11-fluorodibenzo[*a*,*c*]phenazine (EFBPz), were synthesized by coupling fluorodibenzo[*a*,*c*]phenazine (FBPz) with electron rich 3-hexylthiophene and ethylene dioxythiophene (EDOT) units. The monomers were polymerized electrochemically and their electrochemical, spectroelectrochemical and electrochromic behaviors were studied. Then, PTFBPz and PEDOT comprising electrochromic device was constructed and reported. Comparing both polymers in terms of their redox potentials, as expected, PEFBPz showed a lower oxidation potential due to the insertion of an electron rich EDOT unit into the polymer chain, which increased the electron density significantly. EDOT comprising dibenzo[*a*,*c*]phenazine derivative PEFBPz exhibited a red shifted neutral state absorption with lower optical band gap values compared to those of PTFBPz. Furthermore, three novel D–A type dibenzo[*a*,*c*]phenazine comprising polymers (**PBDT-TFBPz**, **PBDT-FBPz** and **PSi-TFBPz**) were synthesized chemically and all polymers were investigated in terms of their electrochromic and physicochemical behaviors.

1. Introduction

After the discovery of conductivity of polyacetylene (PA), conjugated polymers have been accepted as an alternative to inorganic counterparts and used in a variety of applications due to their fascinating properties like low cost fabrication, fabrication of large areas, solution processability and easy control over electronic, organic and physical properties.[1–5] The discovery of these fascinating, multifunctional materials has opened a new research area and several researchers are focused on the field of conjugated polymers and their potential usage in different application areas such as electrochromic devices (ECDs), organic photovoltaics (OPVs), organic light emitting diodes (OLEDs), field effect transistors (FETs), biosensors, and super capacitors (SCs).[6–14]

There are some crucial parameters for conjugated polymers such as the band gap (E_g), absorption in the visible region and energy levels. The Highest Occupied Molecular Orbital (HOMO) and the Lowest Unoccupied Molecular Orbital (LUMO) affect the performance of conducting polymers (CPs) in these applications. For instance, in terms of OSC applications, high performance PSCs require narrow band gaps and suitable energy levels to maximize the short-circuit current (J_{sc}), open-circuit voltage (V_{oc}) and high carrier mobility to facilitate hole transport.[15] In the literature different methods were applied for band gap and energy level modification; however, the D–A approach is one of the most important and widely preferred strategies to broaden the absorption and tune the E_g and energy levels.[16] For that purpose, a variety of D–A copolymers comprising different donor and acceptor units were designed and synthesized to modify the physicochemical properties and obtain high performance ECD and OSCs with high stability.

In the literature, benzoxadiazole, quinoxalines, benzotriazoles, cyanovinylenes, benzimidazoles and benzooxadiazoles are widely preferred acceptor units.[17–22] The quinoxaline unit which is also known as benzopyrazine, is a heterocyclic compound comprising a ring complex that bears a benzene ring and a pyrazine ring. Quinoxaline units possess the advantages

[a] *Department of Basic Sciences of Engineering, Faculty of Engineering and Natural Sciences, Iskenderun Technical University, 31200, Hatay, Turkey. E-mail: serife.hacioglu@iste.edu.tr*
[b] *Department of Chemistry, Middle East Technical University, Ankara 06800, Turkey*
[c] *Department of Chemical, Materials and Production Engineering, University of Naples Federico II, PiazzaleTecchio 80, 80125 Fuorigrotta, Italy*
[d] *ODTU GUNAM, Middle East Technical University, Ankara 06800, Turkey*
[e] *Department of Polymer Science and Technology, Middle East Technical University, 06800 Ankara, Turkey*
[f] *Department of Biotechnology, Middle East Technical University, Ankara 06800, Turkey*

of low cost, easy side chain modification on multipositions, and suitable electron-withdrawing ability to obtain medium-band gap polymers.[23,24] Due to these fascinating properties, quinoxaline derivatives with two electron-withdrawing imine nitrogen atoms have been widely used as the acceptor units during the molecular design of multifunctional CPs especially for ECD and OPV applications.[25] In a recent study, Y. Li and coworkers reported bithienyl-benzodithiophene (BDTT) and difluoroquinoxaline (DFQ) comprising multifunctional D–A type copolymers which were used as donor materials in OPVs achieving a 17.62% power conversion efficiency (PCE).[25] The dibenzo[*a*,*c*]phenazine (DBPz) unit is also a quinoxaline derivative and is accepted as the acceptor unit due to its coplanar structure by connecting the two separated phenyl rings of phenyl-substituted quinoxaline derivatives with a single bond between the *ortho* positions.[26] Additionally, during the molecular design the introduction of the fluorine substituent on the acceptor units has been accepted as a very efficient strategy to improve the PCE of PSCs because fluorine substitution can lower the HOMO/LUMO energy levels to afford a higher open circuit voltage (V_{oc}) and increase the intramolecular polymer chain interaction to obtain a higher hole mobility which resulted in a higher PCE.[27,28] The addition of a strong electron withdrawing pendant group (fluorine atoms) to the polymer backbone significantly influences the electrochemical, optical and electrochromic behaviors of conducting polymers. Z. Xu *et al*. reported that the introduction of fluorine atoms to BT leads to a higher oxidation onset potential, though an improved electrochemical n-doping process.[29] In this study, the DBP unit was also functionalized with the fluorine unit due to the above-mentioned advantages.

During the molecular design, BDT was employed as the electron-rich donor unit due to its rigidity, coplanarity by fusing benzene with two flanking thiophene units, high hole mobility, extended π-conjugated structure and easy side chain modification.[30] In the literature, the BDT unit was widely preferred during the synthesis of both D–A type polymers and small molecules for different means especially for OPV applications.[31–33] In recent years, silole based donor units were also widely used due to the certain advantages of insertion of silicon atoms into the polymer backbone. Insertion of silole units into the polymer backbone resulted in a lower band gap, excellent electron mobility and a low-lying LUMO energy level due to good overlapping between the σ* orbital of the exocyclic silicon–carbon bonds and the π* orbital of the butadiene moiety. Furthermore, recent studies reported that silafluorene (SiF) could be an important functional unit for controlling physicochemical properties of D–A type conducting polymers.[34–37]

Herein, two novel fluorinated dibenzo[*a*,*c*]phenazine derivatives **TFBPz** and **EFBPz** were synthesized. The electrochemically obtained polymers, poly-2,7-bis(5-bromo-4-hexylthiophen-2-yl)-11-fluorodibenzo[*a*,*c*]phenazine (PTFBPz) and poly-2,7-bis(2,3-dihydrothieno[3,4-*b*][1,4]dioxin-5-yl)-11-fluorodibenzo[*a*,*c*]phenazine (PEFBPz), were investigated in terms of their electrochemical, spectroelectrochemical and electrochromic behaviors. Furthermore, fabrication and characterization of PTFBPz/PEDOT comprising an electrochromic device (ECD) were reported. Furthermore, three novel D–A type copolymers namely, poly-2-(4,8-bis((2-ethylhexyl)-oxy)-6-methylbenzo[1,2-*b*:4,5-*b*′]dithiophen-2-yl)-11-fluoro-7-methyl-dibenzo[*a*,*c*]phenazine (**PBDT-TFBPz**), poly-2-(5-(4,8-bis((2-ethylhexyl)oxy)-6-methylbenzo[1,2-*b*:4,5-*b*′]dithiophen-2-yl)-4-hexylthiophen-2-yl)-11-fluoro-7-(4-hexyl-5-methylthiophen-2-yl)dibenzo[*a*,*c*]-phenazine (**PBDT-FBPz**) and poly-11-fluoro-2-(4-hexyl-5-(7-methyl-5,5-dioctyl-5*H*-dibenzo[*b*,*d*]silol-3-yl)thiophen-2-yl)-7-(4-hexyl-5-methylthiophen-2-yl)dibenzo[*a*,*c*]phenazine (**PSi-TFBP**) were synthesized chemically. The aim of designing these polymers is to investigate the effects of fluorine substitution on the optoelectronic properties of dibenzo[*a*,*c*]phenazine derivatives. Furthermore, studies on dibenzo[*a*,*c*]phenazine based polymers for electrochromic applications are limited in the literature. For that reason, the synthesis and electrochromic behaviors of dibenzo[*a*,*c*]phenazine unit containing polymers were reported in this study to make a good contribution to the literature. To show the multipurpose characters of the DBPz unit both electrochemically and chemically obtained polymers were reported.

2. Experimental

2.1. Materials

3-Hexylthiophene, *n*-butyllithium, tributyltinchloride, bis(triphenylphosphine) palladium(II) dichloride, *N*-bromosuccinimide (NBS), 2,6-bis(trimethylstannyl)-4,8-bis(2-ethylhexyloxy)benzo[1,2-*b*:4,5-*b*′]dithiophene (BDT), 9,10 phenanthrenequinone, 4-fluoro-2-nitroaniline, bis(dibenzylideneacetone)palladium(0), and tri(*o*-tolyl)phosphine were purchased from Sigma-Aldrich Chemical Co. Ltd. The $PC_{71}BM$ was purchased from Solenne. Moisture sensitive reactions were conducted under an argon atmosphere. The commodity chemicals were used as received. Tetrahydrofuran (THF) and toluene were dried over Na/benzophenoneketyl and freshly distilled before use.

2.2. Measurements

^1H and ^{13}C NMR spectra were recorded on a Bruker Spectrospin Avance DPX-400 spectrometer with trimethylsilane (TMS) as the internal reference. The chemical shifts were reported in ppm relative to $CDCl_3$ at 7.26 and 77 ppm for the ^1H and ^{13}C NMR, respectively. The UV-Vis spectra were recorded on a Varian Cary 5000 UV-Vis spectrophotometer at room temperature. Cyclic voltammetry studies were carried out in a solution of 0.1 M of tetrabutylammoniumhexafluorophosphate ($TBAPF_6$) in anhydrous acetonitrile (ACN) solution at a scan rate of 100 mV s^{-1} using a Gamry Reference 600 potentiostat in a three-electrode cell consisting of an ITO-coated glass slide as the working electrode, Pt wire as the counter electrode, and Ag wire as the pseudo reference electrode (calibrated against Fc/Fc^+ (0.3 V)). HRMS analyses were performed on a Waters SYNAPT G1 MS instrument. The average molecular weight of the polymer was determined by gel permeation chromatography (GPC) using a Polymer Laboratories GPC 220 with polystyrene as the standard and chloroform as the solvent.

2.3. Synthesis of monomers and polymers

Tributyl(4-hexylthiophen-2-yl)stannane (**6**) and tributyl(2,3-dihydrothieno[3,4-*b*][1,4]dioxin-5-yl)stannane (**7**) were synthesized according to literature procedures.[38–40] Phenanthrene-9,10-dione (**1**) was brominated with *N*-bromosuccinimide (NBS).[41] 4-Fluoro-2-nitroaniline (**3**) was reduced to 4-fluorobenzene-1,2-diamine (**4**) reacted with 2,7-dibromophenanthrene-9,10-dione (**2**) to synthesize 2,7-dibromo-11-fluorodibenzo[*a*,*c*]phenazine (**5**).[42] Compound **5** was coupled with tributyl(4-hexylthiophen-2-yl)stannane (**6**) *via* Stille cross-coupling to afford 11-fluoro-2,7-bis(4-hexylthiophen-2-yl)dibenzo[*a*,*c*]phenazine (**TFBPz**). Bromination of compound **8** was performed in the presence of NBS and $CHCl_3$ to synthesize 2,7-bis(5-bromo-4-hexylthiophen-2-yl)-11-fluorodibenzo[*a*,*c*]phenazine (**9**). Furthermore, compound **5** was coupled with tributyl(2,3-dihydrothieno[3,4-*b*][1,4]dioxin-7-yl)stannane (**7**) *via* Stille cross-coupling to afford 2,7-bis(2,3-dihydrothieno[3,4-*b*][1,4]dioxin-5-yl)-11-fluorodibenzo[*a*,*c*]phenazine (**EFBPz**).

2.3.1. Synthesis of 2,7-dibromophenanthrene-9,10-dione (2). Phenanthrene-9,10-dione (1.0 g, 4.8 mmol) was dissolved in H_2SO_4 (98%) and the flask was surrounded with Al foil paper since NBS is photosensitive. *N*-Bromosuccinimide (2.08 g, 12.0 mmol) was added to solution at room temperature and stirred for 24 h. The acidic reaction mixture was poured into cold water. The orange product was filtered and washed with water to remove acid. After that, it was recrystallized from DMSO to obtain an orange solid product (1.29 g, 73%). ^{1}H NMR (400 MHz, $CDCl_3$) δ 8.24 (s, 2H), 7.78 (s, 4H).

2.3.2. Synthesis of 4-fluorobenzene-1,2-diamine (4). To a solution of 4-fluoro-2-nitroaniline (3.0 g, 19.20 mmol) in ethanol and concentrated hydrochloric acid (37%), tin(II) chloride dihydrate ($SnCl_2{\cdot}2H_2O$) (14.5 g, 76.8 mmol) was added in several portions. The mixture was refluxed for 1 hour and stirred overnight at room temperature. Then, the pH value of the mixture was adjusted to 8–9 by adding aqueous potassium hydroxide (KOH) and then the mixture was extracted three times with ethyl acetate. The combined organic phases were dried over anhydrous magnesium sulfate ($MgSO_4$). The solvent was removed by rotary evaporation. Further purification was performed *via* column chromatography using ethyl acetate as the eluent to give a dark green-brown solid product (1.81 g, 75%). This material was air and light sensitive. ^{1}H NMR (400 MHz, $CDCl_3$) δ 6.55 (dd, J = 8.4, 5.5 Hz, 1H), 6.42–6.25 (m, 2H), 3.29 (d, J = 19.4 Hz, 4H).

2.3.3. Synthesis of 2,7-dibromo-11-fluorodibenzo[*a*,*c*]-phenazine (5). 2,7-Dibromophenanthrene-9,10-dione (1.20 g, 3.27 mmol) and 4-fluorobenzene-1,2-diamine (1.65 g, 13.1 mmol) were dissolved in ethanol. Acetic acid was added to the reaction mixture and refluxed for 1 hour then the reaction mixture was left at room temperature overnight. The mixture was poured into water and the yellow solid was filtered. The product has low solubility; it was washed with chloroform to remove impurities. 2,7-Dibromo-11-fluorodibenzo[*a*,*c*]phenazine was obtained as a yellow solid (0.54 g, 36%). ^{1}H NMR (400 MHz, $CDCl_3$) δ 9.41 (dd, J = 2.17, 5.97 Hz, 2H), 8.28 (t, J = 8.13 Hz, 3H), 7.84 (m, 3H), 7.63 (m, 1H).

2.3.4. Synthesis of 11-fluoro-2,7-bis(4-hexylthiophen-2-yl) dibenzo[*a*,*c*]phenazine (TFBPz). 2,7-Dibromo-11-fluorodibenzo-[*a*,*c*]phenazine (500 mg, 1.09 mmol) (**5**) and tributyl(4-hexylthiophen-2-yl)stannane(1.5 g, 3.30 mmol) (**6**) were dissolved in anhydrous THF. The solution was degassed with argon for 30 minutes and then tris(dibenzylideneacetone) dipalladium(0) (50 mg, 5.5 μmol) and tri(*o*-tolyl)-phosphine (134 mg, 43.6 μmol) were added to the reaction mixture quickly to avoid exposure to oxygen. The reaction temperature was brought to 78 °C and the reaction mixture was stirred overnight. The mixture was extracted with chloroform several times and the solvent was removed by rotary evaporation. The yellow-orange solid was recrystallized from ethanol and pure 11-fluoro-2,7-bis(4-hexylthiophen-2-yl)dibenzo[*a*,*c*]phenazine (560 mg, 81%) was obtained. ^{1}H NMR (400 MHz, $CDCl_3$) δ 9.17 (dd, J = 11.9, 6.0 Hz, 2H), 8.20–8.08 (m, 3H), 7.82–7.68 (m, 3H), 7.55–7.46 (m, 1H), 7.31 (s, 2H), 6.91 (s, 2H), 2.63 (t, J = 7.7 Hz, 4H), 1.67 (m, 6H), 1.41–1.26 (m, 13H), 0.87 (t, J = 6.9 Hz, 6H). ^{13}C NMR (100 MHz, $CDCl_3$) δ 144.45, 143.40, 143.35, 142.42, 142.33, 142.17, 141.15, 139.04, 133.48, 131.45, 131.43, 131.33, 130.26, 129.90, 129.71, 129.51, 127.17, 126.89, 125.12, 125.06, 122.91, 122.12, 122.08, 121.77, 120.34, 120.08, 120.03, 119.94, 31.80, 30.76, 30.51, 29.20, 22.72, 14.16. HRMS (EI) for $C_{40}H_{39}FN_2S_2$ calculated 631.2617, found 631.2611.

2.3.5. Synthesis of 2,7-bis(5-bromo-4-hexylthiophen-2-yl)-11-fluorodibenzo[*a*,*c*]phenazine (9). In a 50 mL two-neck round bottom flask, 11-fluoro-2,7-bis(4-hexylthiophen-2-yl)dibenzo[*a*,*c*]-phenazine (500 mg, 1.04 mmol) was dissolved in chloroform and NBS (366 mg, 2.06 mmol) was added slowly at room temperature and the mixture was stirred for 12 hours. The mixture was extracted with chloroform. Then, the solvent was evaporated under pressure. The dark yellow product was recrystallized from ethanol to obtain the pure product. 2,7-Bis(5-bromo-4-hexylthiophen-2-yl)-11-fluorodibenzo[*a*,*c*]phenazine (375 mg, 60%) was obtained as a dark yellow solid.^{1}H NMR (400 MHz, $CDCl_3$) δ 9.30 (d, J = 5.4 Hz, 2H), 8.38–8.24 (m, 3H), 7.94–7.72 (m, 3H), 7.63–7.56 (m, 1H), 7.23 (s, 2H), 2.59 (t, 4H), 1.64 (m, 4H), 1.43–1.07 (m, 12H), 0.84 (m, 6H).

2.3.6. Synthesis of 2,7-bis(2,3-dihydrothieno[3,4-*b*][1,4]dioxin-5-yl)-11-fluorodibenzo[*a*,*c*]phenazine (EFBPz). 2,7-Dibromo-11-fluorodibenzo[*a*,*c*]phenazine (240 mg, 0.520 mmol) (**5**) and tributyl(2,3-dihydrothieno[3,4-*b*][1,4]dioxin-7-yl)stannane (910 mg, 2.10 mmol) (**7**) were dissolved in dry THF under an argon atmosphere. The solution was degassed with argon for 30 minutes after which tris(dibenzylideneacetone) dipalladium(0) (24 mg, 2.60 μmol) and tri(*o*-tolyl)-phosphine (64 mg, 21.0 μmol) were added. The reaction was heated to 78 °C and stirred for 16 hours. Then, the mixture was extracted with chloroform and brine several times and organic solvent was removed by rotary evaporation. The orange solid was recrystallized using ethanol and pure 2,7-bis(2,3-dihydrothieno[3,4-*b*][1,4]dioxin-5-yl)-11-fluorodibenzo-[*a*,*c*]phenazine was obtained after filtration. ^{1}H NMR (400 MHz, $CDCl_3$) δ 9.45 (dd, J = 10.9, 2.1 Hz, 2H), 8.39–8.18 (m, 3H), 8.04 (dd, J = 8.5, 2.0 Hz, 2H), 7.86 (dd, J = 9.5, 2.8 Hz, 1H), 7.59–7.50 (m, 1H), 6.34 (s, 2H), 4.46–4.19 (m, 8H). HRMS (EI) for $C_{32}H_{19}FN_2O_4S_2$ calculated 579.0849, found 579.0845.

2.3.7. Synthesis of P1(PBDT-FBPz). 2,7-Dibromo-11-fluorodibenzo[*a*,*c*]phenazine (100 mg, 0.210 mmol) and 2,6-bis(trimethylstannyl)-4,8-bis(2-ethylhexyloxy)benzo[1,2-*b*:4,5-*b*0]dithiophene

(178 mg, 0.230 mmol) were dissolved in dry THF and the solution was degassed with argon for 30 minutes. Tris(dibenzylideneacetone) dipalladium(0) (10 mg, 1.1 μmol) and tri(*o*-tolyl)-phosphine (26.6 mg, 84.0 μmol) were added to the reaction medium and refluxed for 24 hours. 2-Bromothiophene (71.4 mg, 0.430 mmol) was added as first end-capper with a small amount of catalyst after 24 hours. Afterwards, tributyl(thiophen-2-yl)stannane (326 mg, 0.870 mmol) was added as a second end-capper with a small amount of catalyst after 30 hours. The solvent of polymerization was removed under reduced pressure and the polymer was precipitated in methanol. To obtain the pure polymer, Soxhlett extraction was carried out with acetone and hexane. The polymer was then dissolved in chloroform and re-precipitated in methanol. When **PBDT-FBPz** dried under vacuum, it was obtained as an orange solid with a yield of 50% (90 mg). GPC: number average molecular weight (M_n): 9400, weight average molecular weight (M_w): 13 200, polydispersity index (PDI): 1.4.

2.3.8. Synthesis of P2 (PBDT-TFBPz). The same procedure as that for the synthesis of **PBDT-FBPz** was applied to synthesize the **PBDT-TFBPz**. 2,7-Bis(5-bromo-4-hexylthiophen-2-yl)-11-fluorodibenzo[*a*,*c*]phenazine (250 mg, 0.31 mmol) and 2,6-bis(trimethylstannyl)-4,8-bis(2-ethylhexyloxy)benzo[1,2-*b*:4,5-*b*0] dithiophene (247 mg, 0.320 mmol) were dissolved in anhydrous THF and the mixture was purged with argon to remove oxygen in the medium. Tris(dibenzylideneacetone) dipalladium(0) (14.2 mg, 1.6 μmol) and tri(*o*-tolyl)-phosphine (37.8 mg, 12.4 μmol) were added to the reaction mixture and the mixture was heated to 78 °C for 24 hours. 2-Bromothiophene (100 mg, 0.620 mmol) and tributyl(thiophen-2-yl)stannane (462 mg, 1.240 mmol) were added to the reaction medium as the end-cappers. The solvent was removed under reduced pressure and the polymer was then precipitated in methanol and extracted sequentially with acetone and hexane. Afterwards the polymer was precipitated in the ethanol to afford a dark-orange solid with a yield of 5% (7 mg). GPC: M_n: 21 700, M_w: 22 500, PDI: 1.1.

2.3.9. Synthesis of P3 (PSi-TFBPz). In a 100 mL two-neck round bottom flask, 2,7-bis(5-bromo-4-hexylthiophen-2-yl)-11-fluorodibenzo[*a*,*c*]phenazine (100 mg, 0.130 mmol), 9,9-dioctyl-9*H*-9-silafluorene-2,7-bis(boronic acid pinacol ester) (92.2 mg, 0.140 mmol) and a catalytic amount of tetrahexyl ammonium iodide (25 mg) was added and the medium was purged with argon for 30 minutes. Then, K_2CO_3 solution (2 M, 0.5 mL) and tetrahydrofuran (THF) were added to the reaction medium. After that, bis(triphenylphosphine)palladium(II) dichloride (4.5 mg, 6.3 μmol) was added and the mixture was heated to 78 °C. The polymerization reaction was continued at this temperature under an argon atmosphere for 24 hours. Bromobenzene (103 mg, 0.656 mmol) and extra catalyst (3.50 mg) were then added and the mixture was stirred for three hours. Then phenyl boronic acid (160 mg, 1.31 mmol) was added and the mixture was stirred at 78 °C overnight. The polymer was precipitated in methanol. Afterwards, the polymer was filtered and extracted with acetone and hexane to remove oligomers and small molecules in a Soxhlett extractor. The polymer was collected with chloroform and the solvent was evaporated. The residue was precipitated in methanol and a red solid polymer with a yield of 15% (35 mg) was obtained. GPC: M_n: 7600, M_w: 20 000, PDI: 2.6 (Schemes 1 and 2).

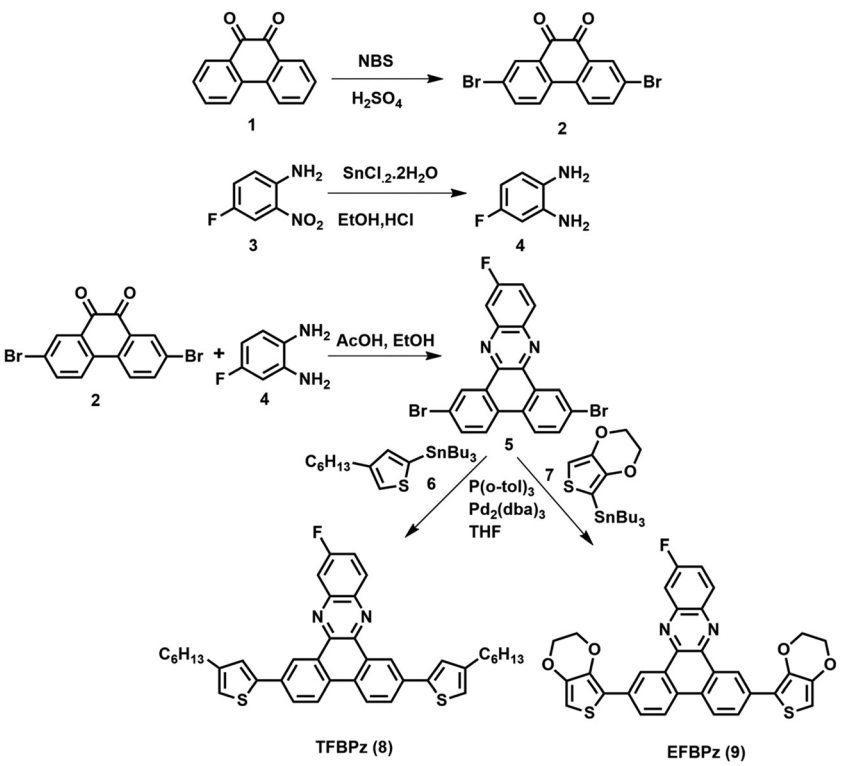

Scheme 1 Synthesis of monomers **TFBPz** and **EFBPz**.

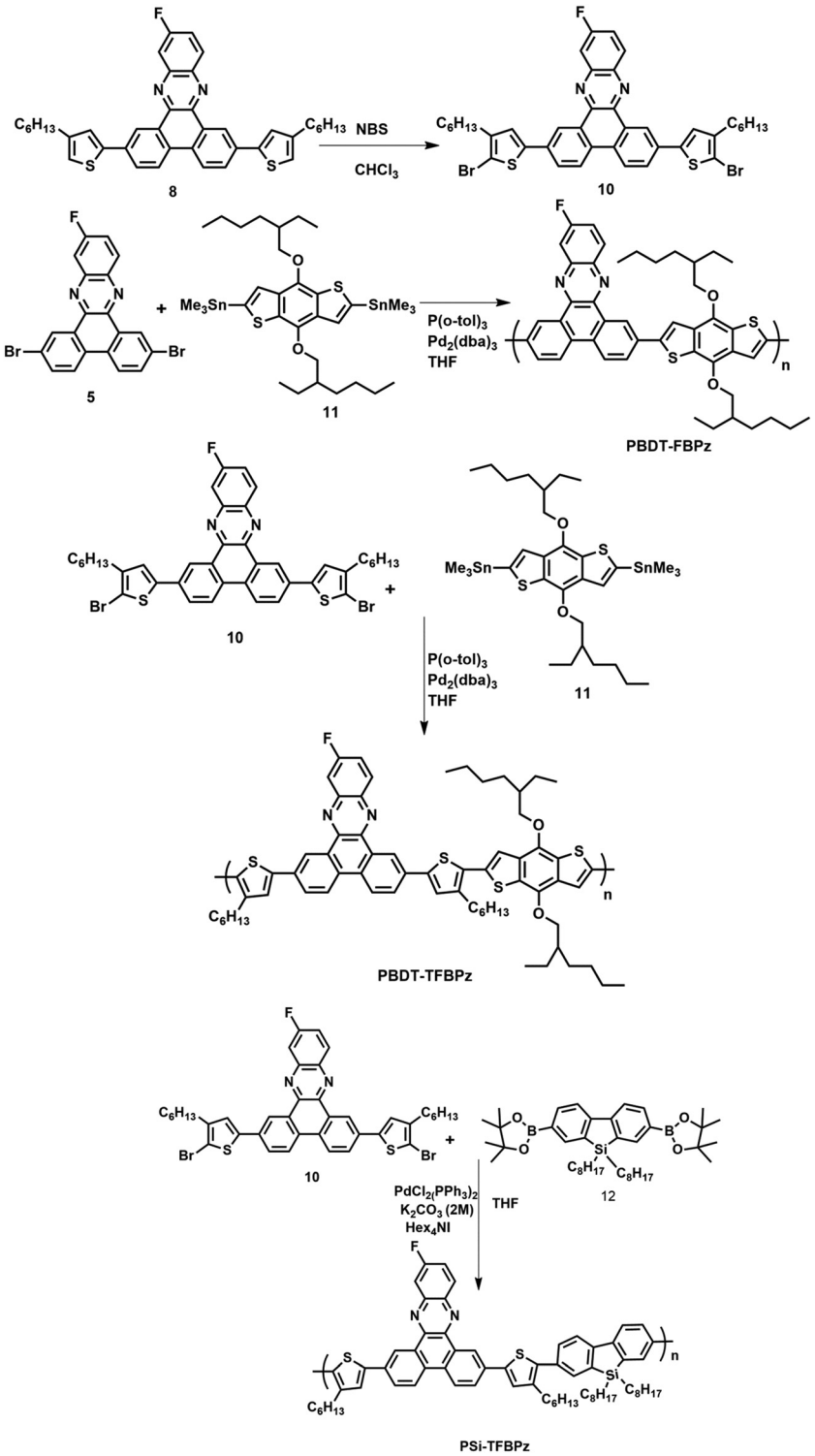

Scheme 2 Synthesis of polymers **PBDT-FBPz**, **PBDT-TFBPz** and **PSi-TFBPz**.

3. Results and discussion

3.1. Electrochemical polymerization and characterization of PTFBPz and PEFBPz films

Cyclic Voltammetry (CV) is a versatile technique that is widely used for the determination of HOMO/LUMO energy levels and oxidation/reduction behaviors of the conjugated polymers. Herein, both electrochemical polymerization and electrochemical characterization were performed *via* CV using a conventional three electrode cell consisting of an ITO coated glass slide as the working electrode, platinum wire as the counter electrode and Ag wire as the pseudo reference electrode. Electrochemical

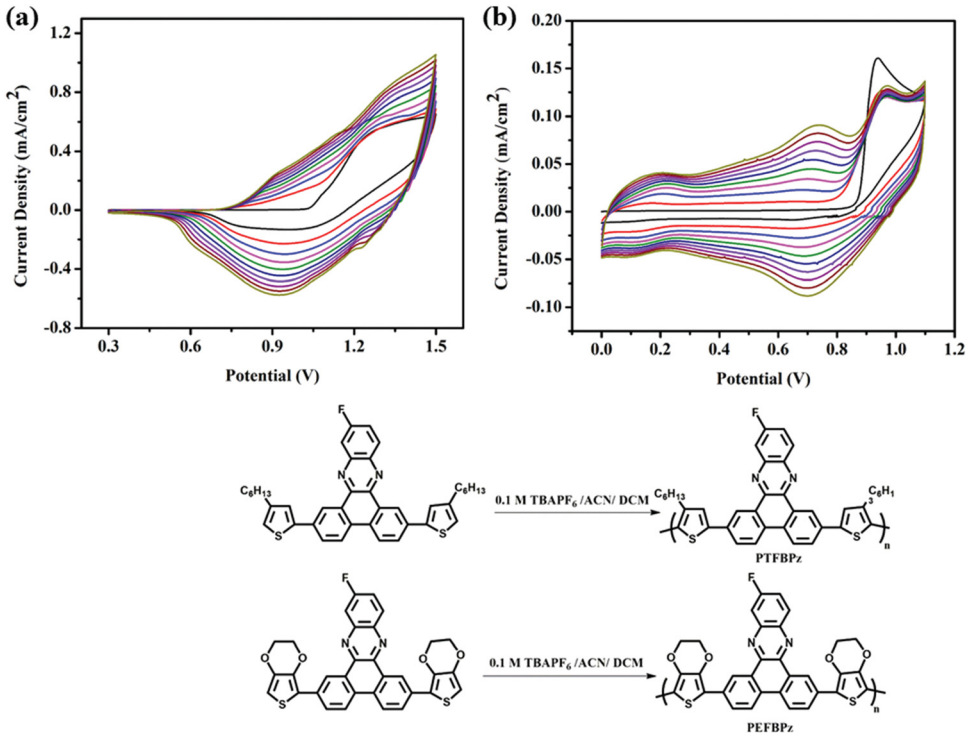

Fig. 1 Electropolymerization of (a) PTFBPz and (b) PEFBPz in 0.1 M $TBAPF_6$/ACN/DCM electrolyte/solvent couple at a 100 mV s^{-1} scan rate.

polymerization of both **TFBPz** and **EFBPz** were performed in 0.1 M tetrabutylammoniumhexafluorophosphate ($TBAPF_6$)-acetonitrile (ACN)/dichloromethane (DCM)/(50/50, v/v), electrolyte–solvent couple at a 100 mV s^{-1} scan rate. The CVs for electrochemical polymerization of **TFBPz** and **EFBPz** and corresponding electropolymerization conditions are depicted in Fig. 1. As seen in Fig. 1, irreversible monomer oxidation peaks were recorded at 1.27 V (**TFBPz**) and 0.94 V (**EFBPz**) in the first cycle of the CVs. Upon sequential cycling, the increase in the peak intensities were observed for both monomers which prove the formation of an electroactive polymer film on the ITO electrodes.

After successive electropolymerization, single scan CVs were recorded for both polymers in a monomer free 0.1 M $TBAPF_6$/ACN solution to investigate the p-doping and n-doping

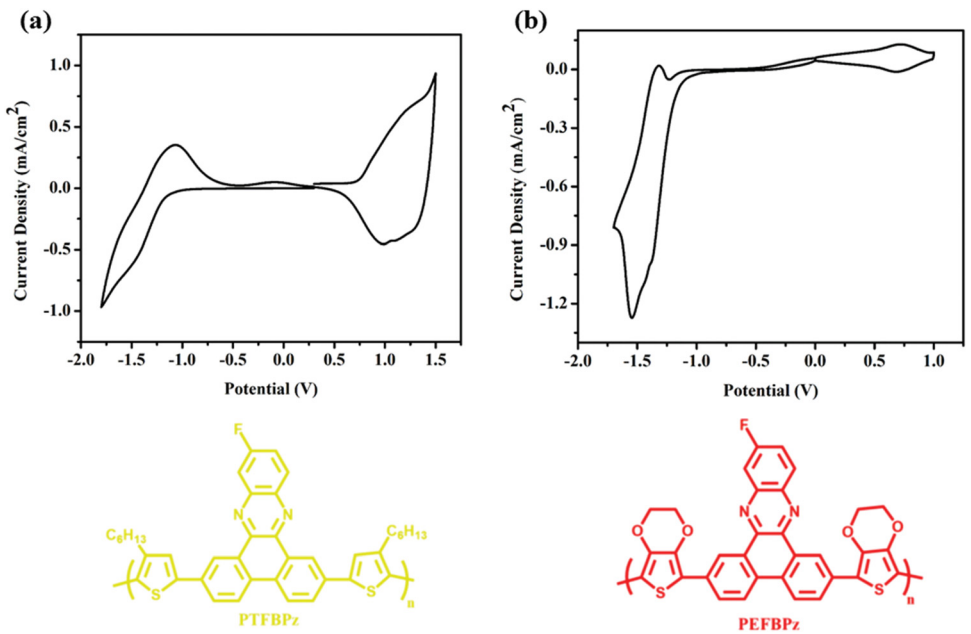

Fig. 2 Single scan cyclic voltammograms of (a) PTFBPz and (b) PEFBPz in 0.1 M $TBAPF_6$/ACN electrolyte/solvent couple.

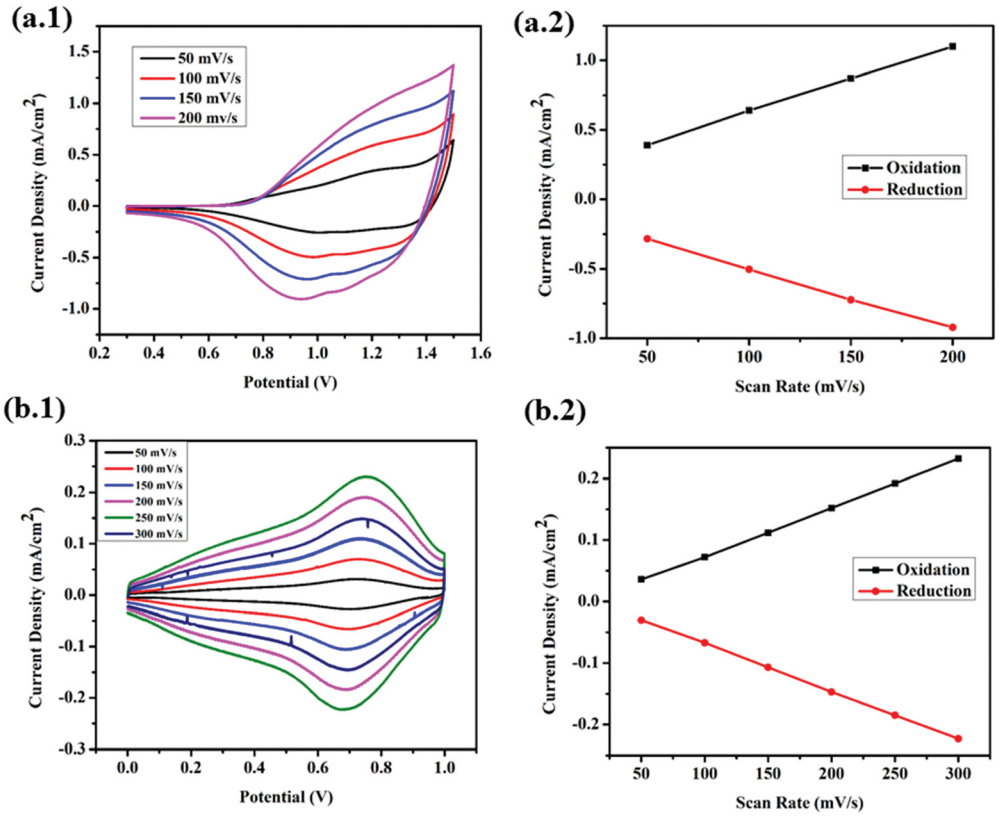

Fig. 3 Scan rate dependence of (a) PTFBPz and (b) PEFBPz in a 0.1 M $TBAPF_6$/ACN solution.

behaviors and to calculate the highest occupied molecular orbital (HOMO) and lowest unoccupied molecular orbital (LUMO) energy levels. Both polymers exhibited an ambipolar character as shown in the Fig. 2 and oxidation potentials of the polymers were recorded at 1.20 V/0.98 V for PTFBPz, 0.72 V/0.68 V for PEFBPz, respectively. Reduction potentials were also calculated from Fig. 2 as −1.43 V/−1.07 V for PTFBPz and −1.55 V/−1.32 V for PEFBPz. Comparing the two polymers in terms of their redox potentials, as expected, PEFBPz showed a lower oxidation potential due to insertion of an electron rich EDOT unit into the polymer chain which increased the electron density significantly.

HOMO/LUMO energy levels of electrochemically synthesized polymers were calculated using eqn (1) and (2) from the onsets of the oxidation/reduction potentials as −5.78 eV/−3.95 eV for PTFBPz and −4.93 eV/−3.92 eV for PEFBPz.

$$\text{HOMO} = -(4.75 + E_{ox}^{onset} - 0.3) \quad (1)$$

$$\text{LUMO} = -(4.75 + E_{red}^{onset} - 0.3) \quad (2)$$

The scan rate dependence of the doping–dedoping process was studied *via* CV. For the study, single scan CVs were recorded at different scan rates as 50 mV s^{-1}, 100 mV s^{-1}, 150 mV s^{-1}, 200 mV s^{-1} for PTFBPz and 50 mV s^{-1}, 100 mV s^{-1}, 150 mV s^{-1}, 200 mV s^{-1}, 250 mV s^{-1}, 300 mV s^{-1} for PEFBPz. The peak current changes of PTFBPz and PEFBPz were monitored by Randles–Sevcik equation (eqn (3)).

$$ip = kAD^{1/2}n^{3/2}C\nu^{1/2} \quad (3)$$

As result of scan rate studies, as seen in Fig. 3, a linear dependence of current density to the scan rate was observed for both polymers. This linear dependence proves that the electro-active polymer films were successfully adhered onto ITO electrodes and the reversible oxidation processes are non-diffusion controlled for both polymers.

3.2. Spectroelectrochemical and kinetic properties of PTFBPz and PEFBPz films

The electronic structure and optical behaviors of PTFBPz and PEFBPz films were studied by spectroelectrochemical measurements in a monomer-free 0.1 M $TBAPF_6$/ACN solution by applying a potential from 0.0 V to +1.5 V for PTFBPz, 0.0 V to +1.0 V for PEFBPz.

As seen in Fig. 4(a.2) and (b.2), the neutral forms of the PTFBPz and PEFBPz films are yellow and light purple in color, having absorbance peaks centered at 353/370 nm and 443 nm, respectively. Before stepwise oxidation, a constant potential at −0.5 V was applied to remove the trapped charge or ion to achieve the true neutral film absorption. As seen in Fig. 4, during stepwise oxidation the intensity of the neutral absorption in the visible region started to decrease and meanwhile new bands arose at around 600 nm and 1100 nm, which proved the formation of charge carriers namely polarons and bipolarons. The optical band gaps of the resulting polymers were calculated from the onset of neutral state λ_{max} values as 2.40 eV for PTFBPz and 1.86 eV for PEFBPz.

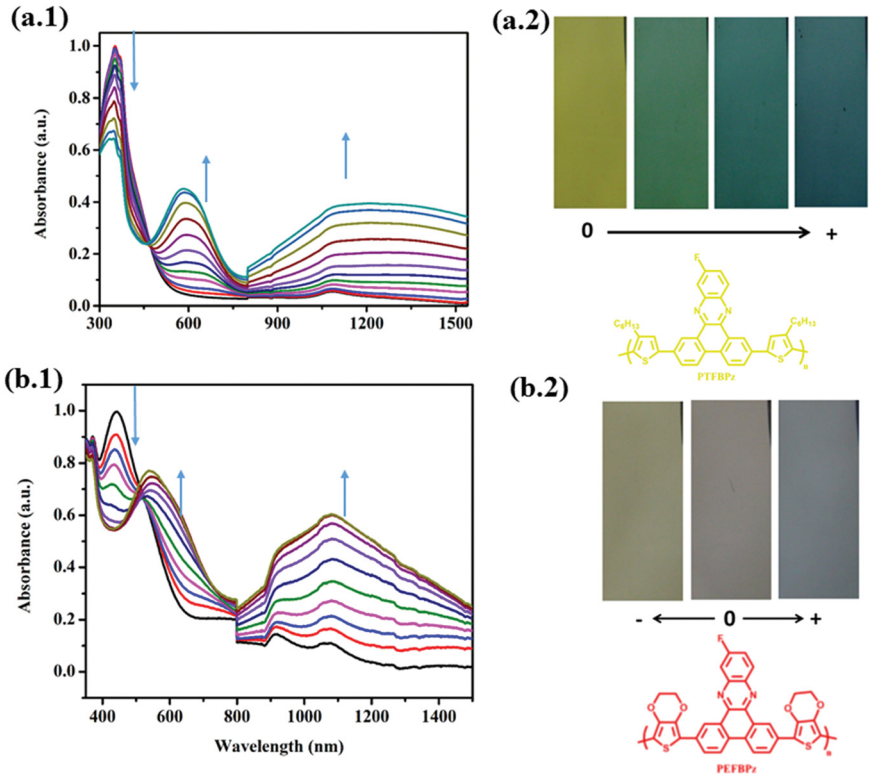

Fig. 4 Spectroelectrochemical behaviors and colors of (a) PTFBPz and (b) PEFBPzin 0.1 M $TBAPF_6$/ACN solution.

Similar to the electrochemical behaviors, insertion of an electron rich EDOT unit into the polymer chain affect the λ_{max} and optical E_g values. As seen in Table 1, EDOT comprising dibenzo[*a*,*c*]phenazine derivative PEFBPz exhibited a red shifted neutral state absorption with lower optical band gap values compared to those of PTFBPz.

The electrochromic switching experiments for both polymer films coated on the ITO electrode were carried out in the visible and NIR regions in 0.1 M $TBAPF_6$/ACN solution. Two consecutive potentials were applied at 0.0 V and +1.5 V for PTFBPz and at 0.0 V and +1.0 V for PEFBPz at regular intervals of 5 s. Optical contrast (*T*%) and response (switching) time are two vital characteristics of electrochromic materials. While the former can be defined as the transmittance difference between the two extreme redox states, the latter one is the necessary time for 95% of the full electrochromic switch between two states (neutral and oxidized). The results of kinetic studies are summarized in Table 2, optical contrasts were calculated as 48% at 600 nm and 85% at 1100 nm with1.6 s and 2.9 s switching times for PTFBPz. Optical contrasts of PEFBPz were detected as 24% at 1120 nm with a fast switching time of 0.5 s (Fig. 5).

Colorimetry studies were performed in order to report the colors in a scientific way. *L*, *a*, and *b* values were reported in Table 3 according to CIE (Commission Internationale de l'Eclairage), where '*L*' represents the brightness of the color, '*a*' represents the color between red/magenta and green and '*b*' represents the color between yellow and blue in the colorimetric measurements. In the neutral state, PTFBPz exhibited a yellow color (*L*: 79, *a*: −9, *b*: 42) and PEFBPz showed a light purple color (*L*: 76, *a*: 1, *b*: 4). The colors of polymers changed upon applied potential; PTFBPz was observed as green (*L*: 60, *a*: −20, *b*: 3) at 1.15 V, turquoise (*L*: 32 *a*: −12, *b*: −6) at 1.25 V and blue (*L*: 47, *a*: −10, *b*: −12) at 1.45 V. The colors of PEFBPz were observed as orange (*L*: 78, *a*: −3, b: 4) at −1.6 V and blue (*L*: 76, *a*: −2, *b*: −6) at 0.75 V in the n-doped and p-doped states, respectively.

Fluoride free analogues of PTFBPz and PEFBPZ were reported previously by Unver *et al.*[41] In the previous study, dibenzo[*a*,*c*]phenazine unit was coupled with 3-hexylthiophene and EDOT groups. 3-Hexylthiophene bearing derivative HTP exhibited yellow color in the neutral state with blue colored oxidized states with a 2.4 eV optical band gap. In this study, 3-hexylthiophene comprising PTFBPz exhibited superior

Table 1 Summary of electrochemical and spectroelectrochemical properties of PTFBPz and PEFBPz

	E_m^{ox} (V)	$E_{p\text{-doping}}$ (V)	$E_{p\text{-dedoping}}$ (V)	$i^p_{n\text{-doping}}$ (V)	$E^p_{n\text{-dedoping}}$ (V)	HOMO (eV)	LUMO (eV)	E_g^{ec} (eV)	λ_{max} (nm)	E_g^{op} (eV)	Polaron/bipolaron
PTFBPz	1.27	1.20	0.98	−1.43	−1.07	−5.78	−3.95	1.83	353/370	2.40	600/1100
PEFBPz	0.94	0.72	0.68	−1.55	−1.32	−4.93	−3.92	1.01	443	1.86	550/1120

Table 2 Optical contrasts and switching times of the PTFBPz and PEFBPz

	Wavelength (nm)	Optical contrast (%)	Switching time (s)
PTFBPz	600	48	1.6
	1100	85	2.9
PEFBPz	1120	24	0.5

Table 3 Colorimetry results of PTFBPz and PEFBPz

Polymers	Potential (V)	*L*	*a*	*b*
PTFBPz	0.00	79	−9	42
	1.15	60	−20	3
	1.25	32	−12	−6
	1.45	47	−10	−12
PEFBPz	−1.60	78	−3	16
	0.00	76	1	4
	0.75	76	−2	−6

electrochemical and optical behaviors compared to the ones in the literature. PTFBP showed yellow and blue colors in the neutral and oxidized states with a multi-electrochromic character and a 2.4 eV optical band gap. While PHTP exhibited 17% optical contrast at 380 nm and 38% optical contrast at 610 nm in the literature, optical contrasts were calculated as 48% at 600 nm and 85% at 1100 nm with 1.6 s and 2.9 s switching times for PTFBPz.

3.3. PTFBPz and PEDOT based ECD fabrication and characterization

Furthermore, prototype solid state double layer PTFBPz and PEDOT bearing an electrochromic device in the ITO/PTFBPz/gel electrolyte/PEDOT/ITO device configuration was fabricated and its properties were examined. For this purpose, electrochemically polymerized PTFBPz and PEDOT were used as anodically and cathodically coloring electrochromic materials. The PTFBPz was electrochemically synthesized on a ITO-coated glass slide as described in the previous parts and ECD was set up in a sandwich configuration in the presence of a gel electrolyte which provides the electron transfer.

The electronic absorption spectra and colors at two extreme states are reported in Fig. 6. As seen, a PTFBPz and PEDOT bearing ECD switches between yellow (at −2.0 V) and blue (at 2.0 V) colors. As seen in Fig. 6(a), spectroelectrochemical studies also demonstrate the colors reported before, with neutral state absorption centered at 390 nm (at −2.0 V) resulting in a yellow color and oxidized state absorption centered at 590 nm (at 2.0 V) which results in blue color.

3.4. Electrochemical and spectroelectrochemical properties of PBDT-FBPz, PBDT-TFBPz and PSi-TFBP

Di-brominated 11-fluorodibenzo[*a*,*c*]phenazine was copolymerized with bis(trimethylstannyl)-4,8-bis(2-ethylhexyloxy)benzo[1,2-*b*:4,5-*b*0]dithiophene and 9,9-dioctyl-9*H*-9-silafluorene-2,7-bis(boronic acid pinacol ester) *via* Stille and Suzuki coupling reactions in order to synthesize **PBDT-FBPz**, **PBDT-TFBPz** and **PSi-TFBP**. Electrochemical and spectroelectrochemical characterizations were performed with CV and UV-Vis-NIR spectrophotometer in order to investigate the redox behaviors, HOMO/LUMO energy levels and band gaps of resulting polymers which are crucial for a variety of applications.

In order to investigate the electronic nature of **PBDT-FBPz**, **PBDT-TFBPz** and **PSi-TFBPz**, the polymers were dissolved in $CHCl_3$ (5 mg mL^{-1}) and spray coated onto an ITO working electrode, and CVs were performed in 0.1 M $TBAPF_6$/ACN solution at a scan rate of 100 mV s^{-1} (Fig. 7). On the anodic scans, polymer oxidation potentials were evolved at 0.95 V for **PBDT-FBPz**, at 1.04 V/1.23 V for **PBDT-TFBPz** and at 1.39 V for **PSi-TFBPz**. While **PBDT-FBPz** and **PSi-TFBPz** had p-type doping behavior, **PBDT-TFBPz** exhibited ambipolar character with a −1.46 V reduction potential. **PBDT-FBPz** and **PBDT-TFBPz** exhibited lower oxidation potentials compared to those of **PSi-TFBPz** which can be attributed to the e-rich nature of the BDT unit and higher M_n values of BDT derivates calculated from GPC analysis.

As reported in Table 4, HOMO/LUMO energy levels of the polymers were calculated from the onset of their oxidation and reduction potentials with respect to the vacuum level of −4.75 eV using eqn (1) and (2). The corresponding HOMO/LUMO energy levels of **PBDT-FBPz**, **PBDT-TFBPz** and **PSi-TFBPz** were determined as −5.41 eV/−3.07 eV, −5.74 eV/−3.94 eV and −5.84 eV/−3.19 eV, respectively.

Spectroelectrochemical analyses are crucial in order to observe the absorption range of the polymers, and E_g values.

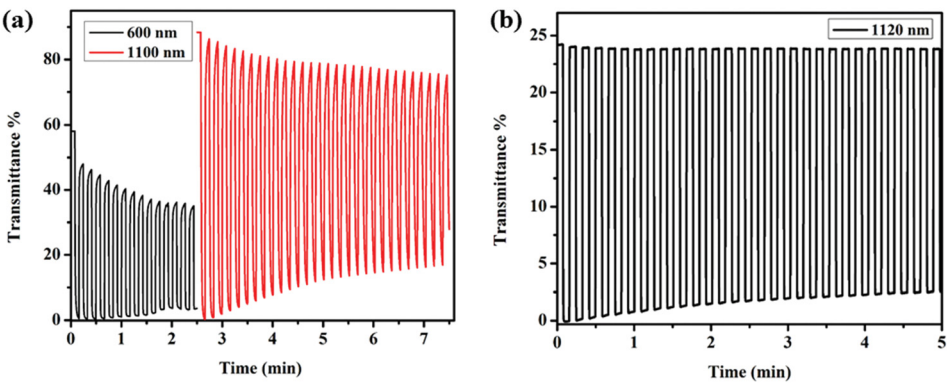

Fig. 5 Percentage transmittance changes and switching times at the maximum wavelengths of (a) PTFBPz and (b) PEFBPz.

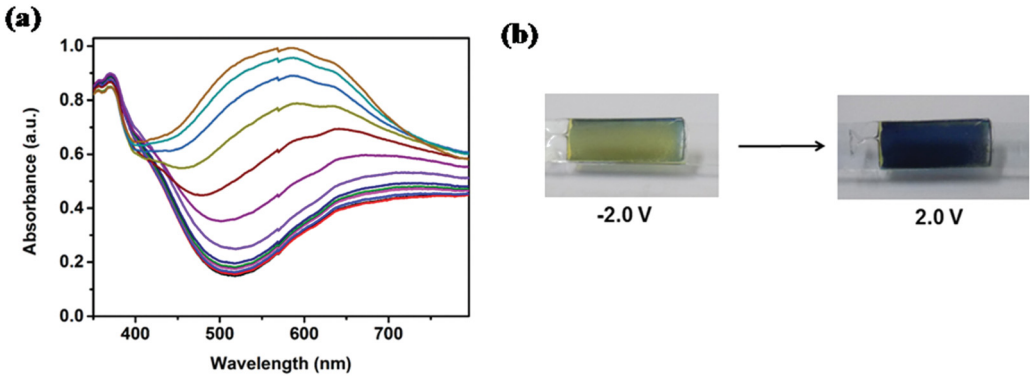

Fig. 6 (a) Spectroelectrochemistry of PTFBPz and PEDOT comprising ECD at applied potentials between −2.0 V and +2.0 V and (b) colors of the ECD.

As a further characterization, spectroelectrochemical characterizations of resulting polymers were investigated *via* gradually increasing the potential in 0.1 M $TBAPF_6$/ACN solution and spectra for **PBDT-TFBPz** and **PSi-TFBPz** were reported in Fig. 8 with the corresponding colors at different redox states. Both polymers were dissolved in chloroform and spray-coated onto ITO electrodes as described before and then a constant potential (−0.5 V) was applied to achieve the true neutral state absorption. During analysis, the potentials were swept stepwise from 0.0 V to 1.2 V for **PBDT-TFBPz** and from 0.0 V to 1.4 V for **PSi-TFBPz**. As seen in Table 4, λ_{max} values for **PBDT-TFBPz** and **PSi-TFBPz** were reported as 454 nm and 375 nm with 1.87 eV and 2.65 eV optical band gap (E_g) values which were calculated from the onset of the lowest energy π–π* transitions.

In terms of colorimetric features, **PBDT-TFBPz** had an orange color (*L*: 71, *a*: 14, *b*: 28) in the neutral state and a gray color (*L*: 67, *a*: −6, *b*: 6) in the oxidized states with green colored (*L*: 68, *a*: −6, *b*: 7) n-doped and green colored (*L*: 68, *a*: −8, *b*: 11) intermediate states. In addition, **PSi-TFBPz** changed its color between yellow (*L*: 74, *a*: −8, *b*: 69) and purple (*L*: 27, *a*: −7, *b*: −22) at the two extreme states with dark green (*L*: 40, *a*: −6, *b*: 18) and dark grey (*L*: 34, *a*: −4, *b*: −1) intermediate colors (Fig. 8).

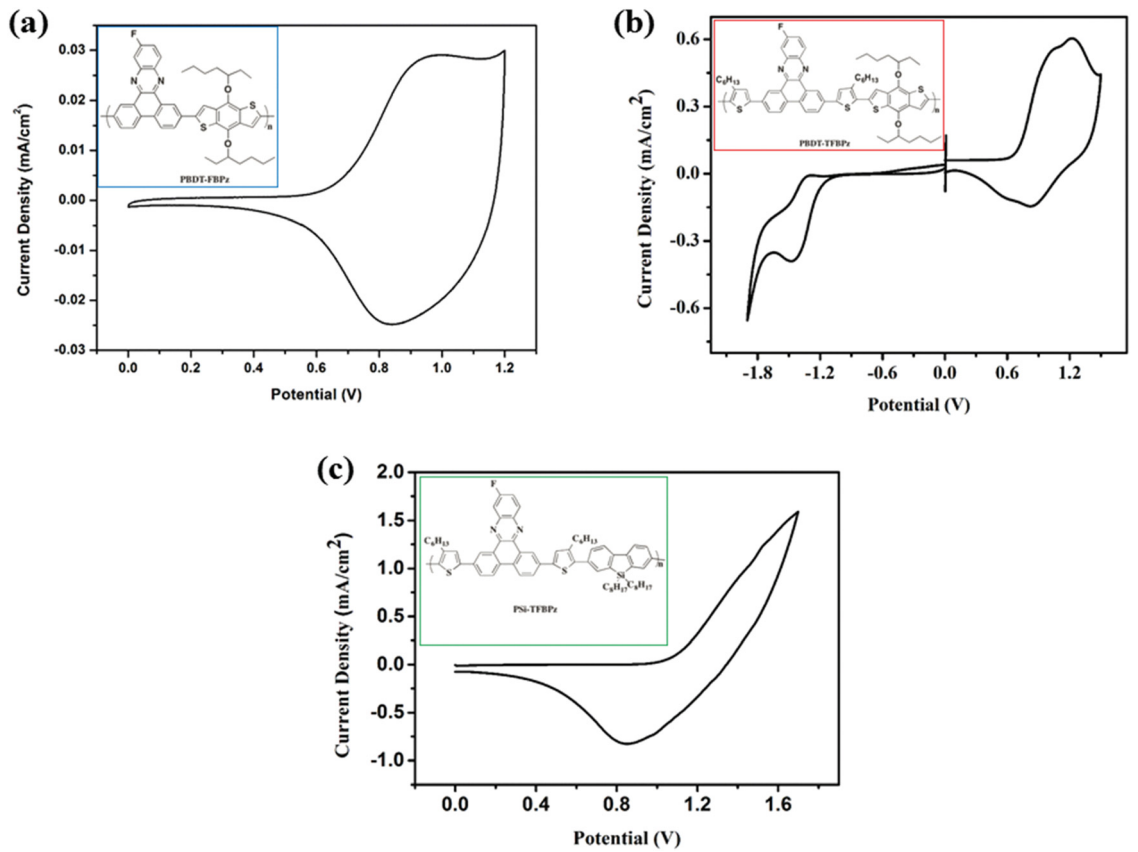

Fig. 7 Single scan CVs of (a) **PBDT-FBPz**, (b) **PBDT-TFBPz** and (c) **PSi-TFBPz** on ITO in 0.1 M $TBAPF_6$/ACN solution at a scan rate of 100 mV s^{-1}.

Table 4 Electronic properties of copolymers (**PBDT-FBPz**, **PBDT-TFBPz** and **PSi-TFBP**)

Copolymers	$E^{p}_{p\text{-doping}}$ (V)	$E^{p}_{p\text{-dedoping}}$ (V)	$E^{p}_{n\text{-doping}}$ (V)	$E^{p}_{n\text{-dedoping}}$ (V)	HOMO (eV)	LUMO (eV)	E^{el}_{g} (eV)	λ_{max} (nm)	E^{op}_{g} (eV)
PBDT-FBPz	0.95	0.80	—	—	−5.41	−3.07	—	380/395	2.34
PBDT-TFBPz	1.04/1.23	0.55/0.83	−1.46	−1.31	−5.74	−3.94	1.80	454	1.87
PSi-TFBPz	1.39	0.86	—	—	−5.84	−3.19	—	375	2.65

In this study, three novel fluorinated dibenzo[*a*,*c*]phenazine comprising conjugated copolymers were designed and synthesized. These polymers have different donor units (BDT and silafluorene) and a fluorine functionalized polymer backbone to decrease the HOMO energy level of polymers to achieve a high V_{oc}. Moreover, 3-hexylthiophene was used as a π-bridge. The added 3-hexylthiophene bridge led to broader absorption. The thiophene bridges would increase the effective conjugation of the polymer chain which results in broader and stronger absorption.[43]

After introducing thiophene bridges in **PBDT-TFBPz**, its LUMO energy level decreased to −3.94 and its HOMO energy level decreased to −5.74 eV as shown in Fig. 9. The increased conjugation on polymer backbone from the thiophene rings is usually expected to give a higher HOMO energy level through improved delocalization of the D–A HOMO wave function. As a result of these substitutions, coplanarity can be increased along the conjugated polymer backbone, and thus an electronic band gap (E^{ec}_{g}) of **PBDT-TFBPz** was observed, lower than that of **PBDT-FBPz**.[44]

Fig. 9 shows the energy level diagram of polymers and OPV materials. As depicted in Fig. 9, energy levels of the polymers are suitable for organic solar cells construction. Thus, **PBDT-FBPz**, **PBDT-TFBPz** and **PSi-TFBP** are promising candidates for organic solar cell applications.

These chemically obtained polymers **PBDT-FBPz**, **PBDT-TFBPz** and **PSi-TFBP** were designed and synthesized for further studies and applications. The reported applications are preliminary studies and also these polymers could be used for OPV applications as a separate study. Furthermore, in the literature number of studies on dibenzo[*a*,*c*]phenazine comprising polymers and their electrochromic applications are limited. For that reason, the synthesis of the dibenzo[*a*,*c*]phenazine unit was reported in this study to make a contribution to the literature. To show the multipurpose characters of the DBPz unit both electrochemically and chemically obtained polymers were reported.

The long term stability measurements for PTFBPz and PEFBPz were recorded and are reported in Fig. 10. For the stability measurements, CVs were recorded in the first cycle and after 100 cycles. As seen, while PTFBPz retains 63% of its

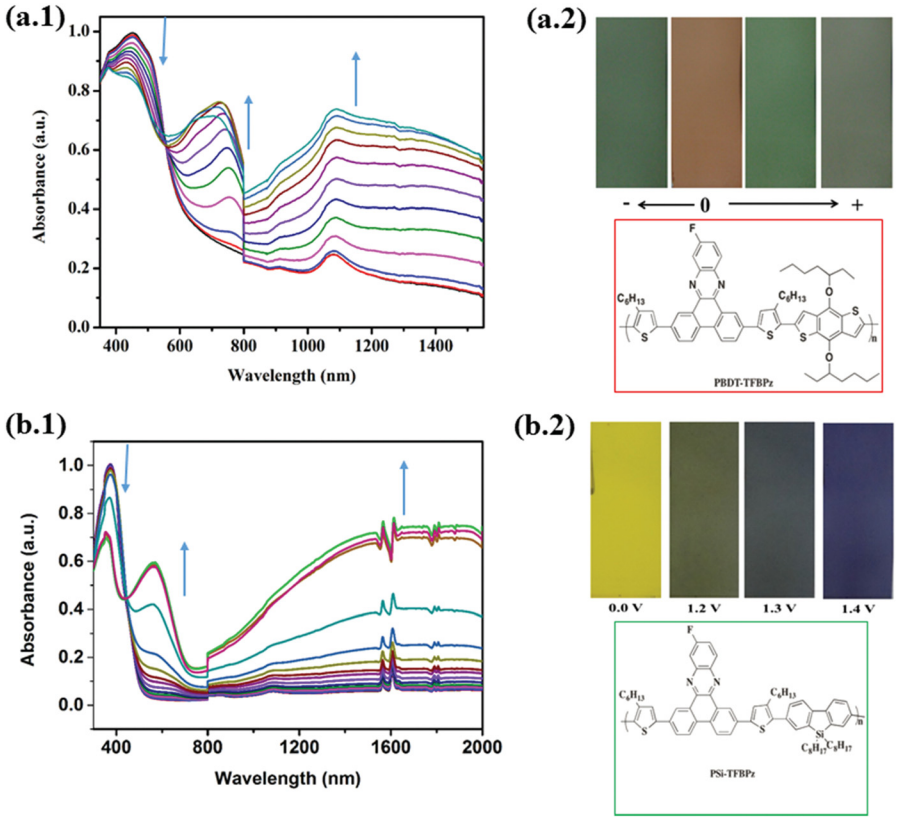

Fig. 8 Change in the electronic absorption spectra of (a) **PBDT-TFBPz**, (b) **PSi-TFBP** and colors of polymers at reduced and oxidized states.

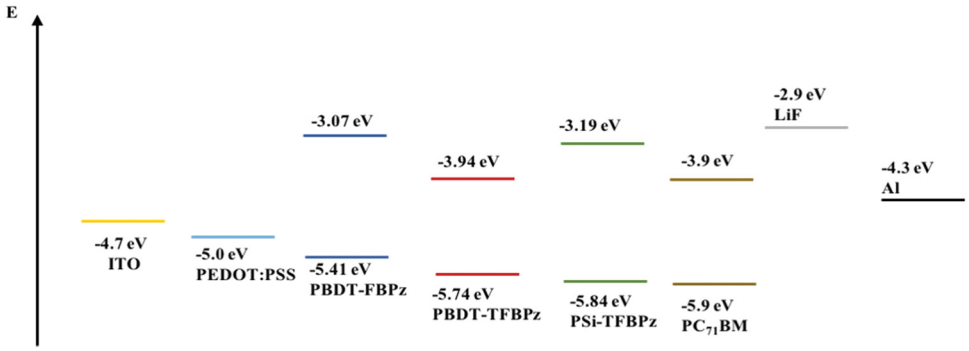

Fig. 9 Energy level diagrams of copolymers (**PBDT-FBPz**, **PBDT-TFBPz** and **PSi-TFBP**) and OPV materials.

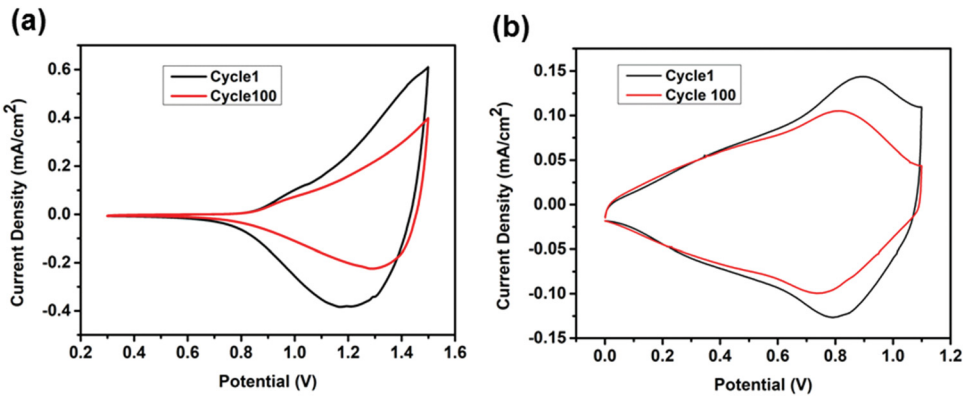

Fig. 10 The long term stability measurements for (a) PTFBPz and (b) PEFBPz.

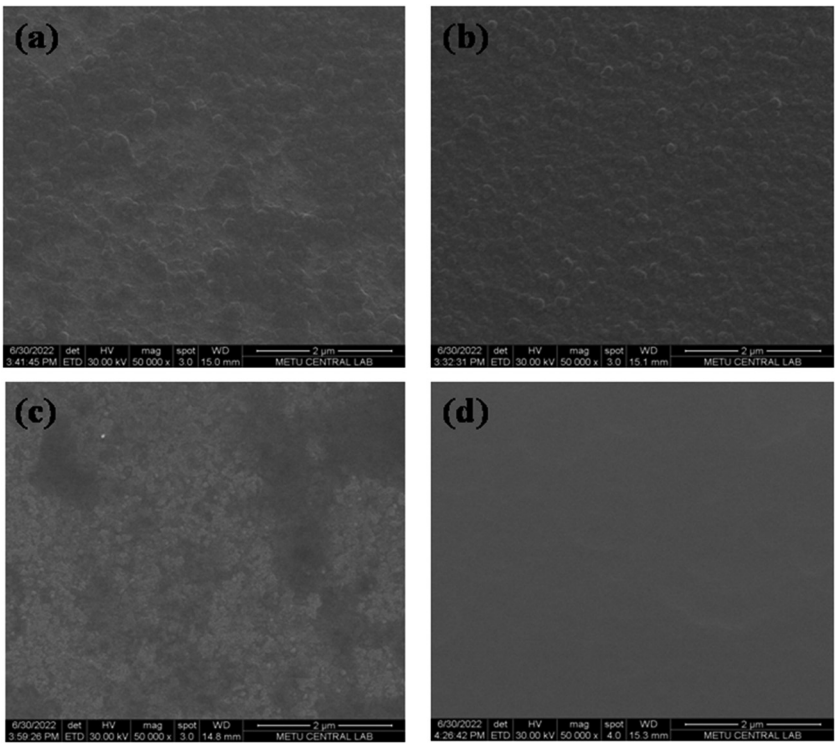

Fig. 11 Surface characteristics (SEM images) of electrochemically obtained polymer films (a) PTFBPz, (b) PEFBPz and chemically obtained polymer films, (c) **PBDT-TFBPz**, (d) **PSi-TFBP** on an ITO electrode.

electro-activity, PEFBPz retains 79% its electro-activity after 100 cycles. As expected, EDOT bearing derivative PEFBPz has higher long term stability which is also consistent with the electrochemical studies.

The morphologies of electrochemically obtained polymer films PTFBPz, PEFBPz and chemically obtained polymer films **PBDT-TFBPz**, **PSi-TFBP** on an ITO electrode were investigated by scanning electron microscopy (SEM) (Fig. 11). All polymer films reveal a uniform surface morphology, which proves that the polymers were homogeneously spread over the electrode surface.

4. Conclusions

In this study, two novel conjugated polymers with electron accepting segments of different FBPz and electron donating segments of 3-hexylthiophene and EDOT were successfully designed and synthesized electrochemically. The electrochemically obtained polymers were compared in terms of their electrochemical and spectroelectrochemical properties. As expected, the electron rich EDOT bearing PBPz derivative PEFBPz showed a lower oxidation potential. Similar to the electrochemical behaviors, insertion of the electron rich EDOT unit into the polymer chain affects λ_{max} and optical band gap (E_g) values and PEFBPz exhibited a red shifted neutral state absorption at 443 nm with a lower optical band gap (1.86 eV) compared to those of PTFBPz. Furthermore, the prototype of solid state double layer PTFBPz and PEDOT comprising the electrochromic device was fabricated and its properties were examined. ECD works between yellow (at −2.0 V) and blue (at 2.0 V) colors with neutral state absorption centered at 390 nm (at −2.0 V) resulting in yellow color and oxidized state absorption centered at 590 nm (at 2.0 V) which results in blue color.

Then, three novel D–A type dibenzo[*a*,*c*]phenazine comprising polymers (**PBDT-TFBPz**, **PBDT-FBPz** and **PSi-TFBPz**) were designed synthesized chemically and the effects of fluorine substitution on the optoelectronic properties were investigated. As a result of spectroelectrochemical studies, λ_{max} values for **PBDT-TFBPz** and **PSi-TFBPz** were reported as 454 nm and 375 nm with 1.87 eV and 2.65 eV optical band gap (E_g) values. In terms of colorimetric features, **PBDT-TFBPz** had orange color and gray color in the neutral and oxidized states. **PSi-TFBPz** changed its color between yellow and purple at the two extreme states with dark green and dark grey intermediate colors. All polymers showed good electrochemical, spectroelectrochemical behaviors with promising electrochromic device properties which make FBPz derivatives multipurpose new generation materials.

Conflicts of interest

There are no conflicts to declare.

References

1 C. K. Chiang, C. R. Fincher, Y. W. Park, A. J. Heeger, H. Shirakawa, E. J. Louis, S. C. Gau and A. G. MacDiarmid, *Phys. Rev. Lett.*, 1977, **39**(17), 1098–1101.
2 S. Qia, C. Wang, Z. Liuc, Y. Hand, F. Baia and Z. Chen, *Dyes Pigm.*, 2022, **204**, 110432.
3 X. Guo and A. Facchetti, *Nat. Mater.*, 2020, **19**, 922–928.
4 M. Hui Chua, S. Heng GeraldToh, P. JinOng, Z. MaoPng, Q. Zhu, S. Xiong and J. Xu, *Polym. Chem.*, 2022, **13**, 967–998.
5 C. J. Brabec, S. Gowrisanker, J. J. M. Halls, D. Laird, S. Jia and S. P. Williams, *Adv. Mater.*, 2010, **22**, 3839–3856.
6 H. Fu, S. Yan, T. Yang, M. Yin, L. Zhang, X. Shao, Y. Dong, W. Li and C. Zhang, *Chem. Eng. J.*, 2022, **438**, 135455.
7 B. Fan, D. Zhang, M. Li, W. Zhong, Z. Zeng, L. Ying, F. Huang and Y. Cao, *Sci. China: Chem.*, 2019, **62**, 746–752.
8 H. Wang, M. Barrett, B. Duane, J. Gu and F. Zenhausern, *Mater. Sci. Eng., B*, 2018, **228**, 167–174.
9 H. Yue, X. Ju, Y. Du, Y. Zhang, H. Du, J. Zhao and J. Zhang, *Org. Electron.*, 2021, **95**, 106183.
10 C. Li, Y. Xu, Y. Liu, Z. Ren, Y. Ma and S. Yan, *Nano Energy*, 2019, **65**, 104057.
11 D. Yigit, M. Gullu, T. Yumak and A. Sınag, *J. Mater. Chem. A*, 2014, **2**, 6512–6524.
12 P. Wang, Y. Sun, J. Li, W. Kang, G. Zhu, H. Zhang, X. Zhang, H. Yang and B.-P. Lin, *New J. Chem.*, 2021, **45**, 18472–18481.
13 W. Fu, H. Chen, Y. Han, W. Wang, R. Zhang and J. Liu, *New J. Chem.*, 2021, **45**, 19082–19087.
14 H. L. T. Mai, N. T. T. Truong, T. Q. Nguyen, B. K. Doan, D. H. Tran, L.-T. T. Nguyen, W. Lee, J. W. Jung, M. H. Hoang, H. P. K. Huynh, C. D. Tran and H. T. Nguyen, *New J. Chem.*, 2020, **44**, 16900–16912.
15 T. Hu, L. Han, M. Xiao, X. Bao, T. Wang, M. Sun and R. Yang, *J. Mater. Chem. C*, 2014, **2**, 8047–8053.
16 J. Roncali, *Macromol. Rapid Commun.*, 2007, **28**, 1761–1775.
17 Q. QusainAfzal, K. Jaffar, M. Ans, J. Rafique, J. Iqbal, R. AqilShehzad and M. ShabirMahr, *Polymer*, 2022, **238**, 124405.
18 M. Changa, Y. Zhang, B.-S. Lu, D. Sui, F. Wang, J. Wang, Y. Yang and B. Kan, *Chem. Eng. J.*, 2022, **427**, 131473.
19 N. A. Unlu, S. O. Hacioglu, G. Hizalan, D. E. Yildiz, L. Toppare and A. Cirpan, *J. Electrochem. Soc.*, 2017, **164**, G71–G76.
20 M. H. Chua, Q. Zhu, T. Tang, K. W. Shah and J. Xuac, *Sol. Energy Mater. Sol. Cells*, 2019, **197**, 32–75.
21 T.-T. Do, K. Matsuki, T. Sakanoue, F.-L. Wong, S. Manzhos, C.-S. Lee, J. Bell, T. Takenobu and P. Sonara, *Org. Electron.*, 2019, **70**, 14–24.
22 A. C. Ozelcaglayan, M. Sendur, N. Akbasoglu, D. H. Apaydin, A. Cirpan and L. Toppare, *Electrochim. Acta*, 2012, **67**, 224–229.
23 J. Yuan, J. Ouyang, V. Cimrová, M. Leclerc, A. Najari and Y. Zou, *J. Mater. Chem. C*, 2017, **5**, 1858–1879.
24 T. Wang, T.-K. Lau, X. Lu, J. Yuan, L. Feng, L. Jiang, W. Deng, H. Peng, Y. Li and Y. Zou, *Macromolecules*, 2018, **51**, 2838–2846.
25 C. Zhu, L. Meng, J. Zhang, S. Qin, W. Lai, B. Qiu, J. Yuan, Y. Wan, W. Huang and Y. Li, *Adv. Mater.*, 2021, **33**, 2100474.
26 R. He, L. Yu, P. Cai, F. Peng, J. Xu, L. Ying, J. Chen and W. Yang, and Yong Cao, *Macromolecules*, 2014, **47**, 2921–2928.

27 H. J. Son, W. Wang, T. Xu, Y. Liang, Y. Wu, G. Li and L. Yu, *J. Am. Chem. Soc.*, 2011, **133**, 1885–1894.
28 A. C. Stuart, J. R. Tumbleston, H. Zhou, W. Li, S. Liu, H. Ade and W. You, *J. Am. Chem. Soc.*, 2013, **135**, 1806–1815.
29 Z. Xua, H. Dub, M. Yina, B. Wanga, J. Zhaob and Y. Xie, *Org. Electron.*, 2018, **61**, 1–9.
30 L. Huo and J. Hou, *Polym. Chem.*, 2011, **2**, 2453–2461.
31 J. Subbiah, B. Purushothaman, M. Chen, T. Qin, M. Gao, D. Vak, F. H. Scholes, X. Chen, S. E. Watkins, G. J. Wilson, A. B. Holmes, W. W. H. Wong and D. J. Jones, *Adv. Mater.*, 2015, **27**, 702–705.
32 G. Li, X. Gong, J. Zhang, Y. Liu, S. Feng, C. Li and Z. Bo, *ACS Appl. Mater. Interfaces*, 2016, **8**(6), 3686–3692.
33 D. Liu, W. Zhao, S. Zhang, L. Ye, Z. Zheng, Y. Cui, Y. Chen and J. Hou, *Macromolecules*, 2015, **48**(15), 5172–5178.
34 C. Duan, W. Cai, F. Huang, J. Zhang, M. Wang, T. Yang, C. Zhong, X. Gong and Y. Cao, *Macromolecules*, 2010, **43**, 5262–5268.
35 G. Li, C. Kang, X. Gong, J. Zhang, W. Li, C. Li, H. Dong, W. Hu and Z. Bo, *J. Mater. Chem. C*, 2014, **2**, 5116–5123.
36 O. Erlik, N. A. Unlu, G. Hizalan, S. O. Hacioglu, S. Comez, E. D. Yildiz, L. Toppare and A. Cirpan, *J. Polym. Sci., Part A: Polym. Chem.*, 2015, **53**, 1541–1547.
37 M. Yuan, P. Yang, M. M. Durban and C. K. Luscombe, *Macromolecules*, 2012, **45**, 5934–5940.
38 C.-Y. Kuo, Y.-C. Huang, C.-Y. Hsiow, Y.-W. Yang, C.-I. Huang, S.-P. Rwei, H.-L. Wang and L. Wang, *Macromolecules*, 2013, **46**, 5985–5997.
39 C. Istanbulluoglu, S. Göker, G. Hizalan, S. O. Hacioglu, Y. ArslanUdum, E. D. Yildiz, A. Cirpan and L. Toppare, *New J. Chem.*, 2015, **39**, 6623–6630.
40 S. S. Zhu and T. M. Swager, *J. Am. Chem. Soc.*, 1997, **119**(51), 12568–12577.
41 E. K. Unver, S. Tarkuc, Y. A. Udum, C. Tanyeli and L. Toppare, *J. Polym. Sci., Part A: Polym. Chem.*, 2010, **48**(8), 1714–1720.
42 S. Kothavale, W. Jae Chung and J. Yeob Lee, *J. Mater. Chem. C*, 2020, **8**, 7059–7066.
43 X. Wang, P. Jiang, Y. Chen, H. Luo, Z. Zhang, H. Wang, X. Li, G. Yu and Y. Li, *Macromolecules*, 2013, **46**, 4805–4812.
44 L. Pandey, C. Risko, J. E. Norton and J.-L. Brédas, *Macromolecules*, 2012, **45**, 6405–6414.